Quantum-Dot-Spin Single-Photon Interface

S. T. Yılmaz, P. Fallahi, and A. Imamoğlu

Institute of Quantum Electronics, ETH Zurich, CH-8093 Zürich, Switzerland
(Received 26 March 2010; revised manuscript received 24 May 2010; published 15 July 2010)

Using background-free detection of spin-state-dependent resonance fluorescence from a single-electron charged quantum dot with an efficiency of 0.1%, we realize a classical single spin-photon interface where the detection of a scattered photon with 300 ps time resolution projects the quantum dot spin to a definite spin eigenstate with fidelity exceeding 99%. The bunching of resonantly scattered photons reveals information about electron spin dynamics. High-fidelity fast spin-state initialization heralded by a single photon enables the realization of quantum information processing tasks such as nondeterministic distant spin entanglement. Given that we could suppress the measurement backaction to well below the natural spin-flip rate, realization of a quantum nondemolition measurement of a single spin could be achieved by increasing the fluorescence collection efficiency by a factor exceeding 10 using a photonic nanostructure.

Optical excitations of an electron spin confined in self-assembled quantum dots (QD) have favorable selection rules that allow for recycling trion transitions where the scattered photon polarization is strongly correlated with the electron spin-state [1]. Realization of a spin-photon interface in the spirit of what has been recently realized for trapped ions [2], however, suffers from the fact that the background laser scattering overwhelms the QD resonance fluorescence (RF). While single QD RF has been recently observed by several groups [3,4], the reported experiments did not demonstrate a complete suppression of the background in a charge-controlled QD that is essential for the realization of a spin-photon interface.

In this Letter, we demonstrate background-free detection of single QD RF with an efficiency of 0.1%. We show that detection of a single photon, resonantly scattered on the charged-exciton (trion) resonance, projects the QD spin to a state where the spin is pointing along the external magnetic field ($|{\uparrow}\rangle$) with a conditional initialization fidelity of 99.2%. Our results constitute a first step towards the realization of nondeterministic spin-spin-entanglement [5,6] schemes. Given that we operate in a regime where measurement backaction in the form of spin-flip Raman scattering rate is weaker than the spin-flip rate induced by coupling to a fermionic reservoir, our results also constitute a first step towards quantum nondemolition (QND) measurement [7] of a single solid-state spin. We estimate that either by identifying QDs with a small heavy-light-hole mixing [8] or by embedding a QD in a two dimensional photonic crystal structure [9] or a microcavity [10–12], it will be possible to realize a QND measurement.

The experiments are carried out with self-assembled InGaAs QDs embedded in a Shottky diode heterostructure which enables deterministic loading of electrons from a nearby Fermi sea separated by a 35 nm thick blocking barrier. The sample is studied using a diffraction limited confocal microscope housed in a liquid-helium bath cryostat at 4.2 K. A single QD is addressed using a laser that is tuned into resonance with its fundamental trion resonance. A magnetic field B is applied in the Faraday configuration. A zirconium solid immersion lens (SIL) is used to improve the collection efficiency.

Figure 1(a) illustrates the relevant QD energy levels. A single electron resides either in the spin-up $|{\uparrow}\rangle$ or spin-down $|{\downarrow}\rangle$ eigenstate. The two optically excited (trion) states $|{\uparrow}{\downarrow}{\Uparrow}\rangle$ and $|{\uparrow}{\downarrow}{\Downarrow}\rangle$ have two electrons in the singlet state and a heavy-hole, either in the (pseudo) spin-up $|{\Uparrow}\rangle$ or spin-down $|{\Downarrow}\rangle$ state. The two ground and excited states are split by the Zeeman energies $|g_e|\mu_B B$ and $|g_h|\mu_B B$. The optical selection rules in the Faraday geometry are such that a right (left)-hand circularly polarized optical field drives the transition $|{\uparrow}\rangle \leftrightarrow |{\uparrow}{\downarrow}{\Uparrow}\rangle$ ($|{\downarrow}\rangle \leftrightarrow |{\uparrow}{\downarrow}{\Downarrow}\rangle$) with the Rabi frequency Ω_R (Ω_L). Spontaneous emission from the trion state occurs with rate $\Gamma \sim 10^9 \text{ s}^{-1}$ and is circularly polarized. The selection rules are relaxed by the ground state mixing due to hyperfine interaction of the electron with the nuclei and by the heavy-light-hole mixing, resulting in weak diagonal transitions with rate γ. For the experiments re-
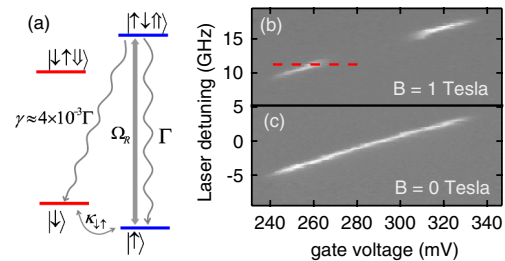

FIG. 1 (color online). (a) Energy level diagram for a quantum dot (QD) charged with a single electron. (b),(c) Differential transmission (DT) signal as a function of gate voltage and laser frequency at $B = 1$ T and $B = 0$ T. At $B = 0$ T, DT signal is seen at gate voltages where the QD is singly charged. At $B = 1$ T the DT signal (white points) in the middle of the plateau disappears due to spin pumping. The dashed line corresponds to the gate voltage trace in Fig. 2(a).

ported here at $B = 1$ T the branching ratio $\frac{\gamma}{\gamma + \Gamma}$ is measured to be $\sim 4 \times 10^{-3}$. Because of the interaction with the electrons in the Fermi sea, electron spin-flip events occur with a cotunneling rate $\kappa_{\uparrow\downarrow}$; this rate can be tuned by more than 6 orders of magnitude from 10^7 s^{-1} to about 10^1 s^{-1} by changing the gate voltage [13].

To determine the transition energies of the QD, differential transmission (DT) measurements are carried out, where the transmitted field is recorded with a photodiode directly under the sample. In the experiments presented here, we have only addressed the higher energy (blue) trion transition $|\uparrow\rangle \leftrightarrow |\uparrow\downarrow\Uparrow\rangle$ with a resonant laser field; provided that $B > 0.2$ T, excitation of the $|\downarrow\rangle \leftrightarrow |\downarrow\uparrow\Downarrow\rangle$ transition can be safely neglected. Figures 1(b) and 1(c) show the DT signal from the trion transition with a 100 ms integration time at $B = 1$ T and $B = 0$ T. The linear increase in the transition energy with increasing gate voltage is due to dc-Stark effect. In the middle of the single-electron plateau the DT signal disappears at $B = 1$ T due to laser induced spin pumping [14]. At the plateau edges, high cotunneling rate ensures the randomization of the electron spin population. The broadening of the absorption line shape for gate voltages where the DT signal starts to disappear is due to dynamical nuclear spin polarization [15].

To realize background free detection of RF using an APD in the Geiger mode, we place a linear polarizer before the single-mode collection fiber. This polarizer is oriented orthogonal to the laser polarization and extinguishes the reflected laser photons by a factor exceeding 10^6 while eliminating only half of the circularly polarized RF photons. This high level of polarization extinction was possible by ensuring that the deviations from linear polarization in the excitation and collection paths are minimized. Figure 2(a) shows the RF signal as the gate voltage is scanned along the dashed line in Fig. 1(b) with an excitation laser power 10 times below the QD saturation (P_{sat}). The deviation of the RF line shape from the expected Lorentzian is most likely due to the nuclear spin polarization [15], since we observe that for $B = 0$, the RF line shape has a perfect Lorentzian line shape. At the gate voltage when the laser is on resonance with the $|\uparrow\rangle \leftrightarrow |\downarrow\uparrow\Uparrow\rangle$ transition, the ratio of the RF counts to the total photon counts is 0.996 ± 0.001. Taking into account the branching ratio, the fidelity of our conditional state initialization is 0.992 ± 0.001. Based on measured RF counts ($\sim 500\,000/s$) at $B = 0$ T for a laser power above QD saturation and using the measured trion lifetime of ~ 1 ns, we estimate an unprecedented overall QD RF collection efficiency of $\sim 0.1\%$.

Figure 2(b) shows a typical time trace of the APD counts integrated for 200 ns per point as the gate voltage in Fig. 2(a) is kept constant for resonant excitation. Whereas at a given time the absence of a photon detection provides almost no information about the electron spin state, detection of an APD electrical pulse means with a confidence level of 99.2% that the electron is in the $|\uparrow\rangle$ state. Moreover, we can locate the electron spin
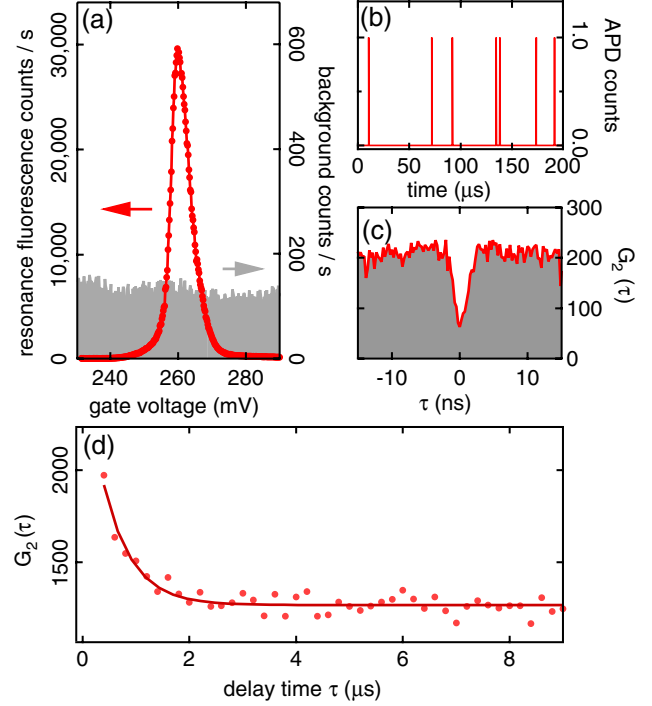

FIG. 2 (color online). (a) Resonance fluorescence (RF) signal from the QD as the gate voltage is scanned along the dashed line on Fig. 1(b). Laser power $P = 0.1 P_{sat}$, where P_{sat} is the power. The gray trace shows the measurement background obtained at the same laser power with the laser frequency fully detuned from the QD transition. On resonance the ratio of RF photons to laser background exceeds 200. (b) A typical time trace recorded from the avalanche photodiode (APD) with a 200 ns time resolution. Each pulse arises from the detection of a single photon. (c) Photon correlation G_2 curve obtained by measuring photon coincidences on two APDs on nanosecond scales. The expected antibunching behavior for a single emitter is observed, with a spontaneous emission rate $\Gamma \sim 10^9$ s^{-1}. The G_2 curve does not reach zero at $\tau = 0$ due to the finite time resolution ~ 450 ps of the Hanbury-Brown and Twiss measurement setup. (d) Long-time G_2 curve obtained from $\sim 60\,000$ traces such as the trace in (b). Solid line is an exponential fit with a decay time $\tau_{decay} = (540 \pm 40)$ nsec, corresponding to the cotunneling-limited spin lifetime.

projection event onto the $|\uparrow\rangle$ state associated with each photon count to within 300 ps of the arrival of the APD pulse; this projection time uncertainty is limited only by the jitter in the rise-time of the APD pulse.

We study RF count statistics by performing second order correlation (G_2) analysis. We first note that the RF photon correlations at short time intervals exhibit the hallmark photon antibunching signature of a single quantum emitter [Fig. 2(c)]. Figure 2(d) shows the unnormalized photon correlation $G_2(\tau)$ curve obtained from $\sim 60\,000$ time traces such as the one shown in Fig. 2(b), at the same gate voltage and laser power. The bunching behavior around $\tau = 0$ reveals information about the spin-flip dynamics. The decay of $G_2(\tau)$, fitted to an exponential function with the decay time $\tau_{decay} = (540 \pm 40)$ ns, provides a direct mea-

surement of the $|\uparrow\rangle$ lifetime. As we discuss below, for the laser power used in this experiment, the laser induced spin decay rate is $(4.4~\mu s)^{-1}$ and the spin lifetime is predominantly determined by cotunneling processes. For the experimental conditions of Fig. 2(b), we estimate that the conditional probability that we detect a photon given that the electron is in $|\uparrow\rangle$ state is $\sim(6.4 \pm 0.6)\%$. By varying the laser intensity the efficiency of spin-state detection can be improved to about 20%; this enhancement comes at the expense of an increase in the laser background such that only 98.6% of the detected photons originate from the QD RF.

In order to prove that the $G_2(\tau)$ decay time is indeed a measure of the spin lifetime, we perform an n-shot measurement [16] of the laser induced spin decay time in the middle of the single-electron plateau where the cotunneling rate is negligible and compare the result to the $G_2(\tau)$ measurements. The n-shot measurement cycle is depicted in the inset of Fig. 3(a): a linearly polarized laser on resonance with the $|\uparrow\rangle \leftrightarrow |\uparrow\downarrow\Uparrow\rangle$ transition is switched on and over a time window of microseconds the RF counts are saved with 200 ns integration time per data point. To undo spin pumping that arises from the spin-measurement backaction in the form of spontaneous spin-flip Raman scattering into the $|\downarrow\rangle$ state, a gate voltage pulse that first ejects the electron from the QD and then injects a new electron with a random spin, is applied. Repeating this cycle $\sim 10\,000$ times at a laser power of $P_{\text{sat}} = 3$ nW, we obtain the n-shot curve depicted in Fig. 3(a) (top curve) with the decay time of (860 ± 20) ns. The decay time of $G_2(\tau)$ obtained with the same laser power and at the same gate voltage is (840 ± 40) ns and is in good agreement with the n-shot measurement [Fig. 3(a) (bottom curve)]. The laser induced decay rates are proportional to the trion population, which in turn is proportional to the RF counts. The measured decay times of (480 ± 30) ns, (860 ± 20) ns, and $(4.4 \pm 0.2)~\mu s$ from the n-shot measurements at laser powers $10P_{\text{sat}}$, P_{sat}, and $0.1P_{\text{sat}}$ agree well with the expected ratio of 1:2:10 (data not shown). Figures 3(b) and 3(c) show $G_2(\tau)$ measurements from another QD performed at two different gate voltages at the edge of the single-electron plateau. In this regime the spin lifetime is determined by the cotunneling processes and the decay of the curves reveals the dependence of the cotunneling rate on the gate voltage.

The realization of a spin-photon interface constitutes a key step towards implementation of quantum information processing protocols such as nondeterministic spin entanglement between distant spins. Even though elimination of laser background through polarization suppression in our scheme results in the loss of correlations between the spin state and the emitted photon polarization, the fact that the photons emitted by the two spin states have different energies ensures that by driving both the red and the blue trion transitions resonantly with a π pulse, we could generate the entangled spin-photon state $|\psi\rangle = (|\uparrow, 1_{\text{blue}}\rangle - |\downarrow, 1_{\text{red}}\rangle)/\sqrt{2}$, starting from an initial electron

spin in state $(|\uparrow\rangle - |\downarrow\rangle)/\sqrt{2}$. As was demonstrated by Monroe and co-workers [6] for two trapped ions, such entangled spin-photon states generated from two distant QDs could be used to achieve spin entanglement conditioned upon coincidence detection of one blue-trion and one red-trion photon at the output of a Hong-Ou-Mandel interferometer. We emphasize that in the nondeterministic entanglement experiments using trapped ions, the entanglement fidelity was primarily limited by the detector dark counts that were $\sim 20\%$ of the signal photons: these considerations highlight the significance of the factor of 20 improvement in the fluorescence to background photon ratio we have achieved in our experiments, as compared to prior work [16]. The principal challenge in realization of the distant QD spin-entanglement scheme is the identification of two QDs with similar enough trion resonances. Even if the two QD trion resonance energies are not exactly identical, it is possible to generate identical QD photons by off-resonant Rayleigh scattering [17]. We emphasize that two-photon interference of single-photon pulses generated by two different QDs has already been demonstrated [18]. Locking of trion resonances to the resonant laser field via dynamical nuclear spin polarization could be used to ensure that the electron Zeeman splitting of the two QDs are rendered identical [15].

The background-free spin-photon interface that we have realized could be considered as a nondeterministic method for conditional spin-state initialization with high fidelity. The deterministic methods for spin-state preparation rely on optical pumping where a fidelity exceeding 99% could only be achieved on a time scale $\sim 10~\mu s$ for Faraday [14] and ~ 10 ns for Voigt geometry [19]. In contrast, detection of a single RF photon in our case prepares the spin state with the same level of initialization fidelity on a time scale limited only by the detector response time [20]. Given the ultrashort $T_2^* \sim 2$ ns characteristic of electron spins in self-assembled QDs [13], fast spin-state initialization is important for protocols relying on preparation of the spin in a superposition state. We also predict that fast spin initialization could be useful in carrying out conditional electron spin resonance (ESR) measurements [21] without the need for a pulsed microwave source; we envision here that the detection of a photon initializes the electron spin in the spin-up state, which then undergoes Rabi oscillations under the influence of the continuous-wave resonant microwave field. The likelihood of detecting a second photon at a time τ later will oscillate with this Rabi coupling, such that photon coincidences at time delay τ will reveal information about coherent spin rotation.

From a quantum measurement perspective, our experiments realize a positive operator valued measure (POVM) with measurement operators $\hat{E}_1 = p_1|\uparrow\rangle\langle\uparrow|$ and $\hat{E}_2 = |\downarrow\rangle\langle\downarrow| + (1 - p_1)|\uparrow\rangle\langle\uparrow|$ [22]. For the parameters of Fig. 2, the probability $p_1 \simeq 0.064$ for a measurement time of $\sim 1.0~\mu s$, but can be increased to 0.2 as mentioned before. If the collection efficiency and the excitation laser power
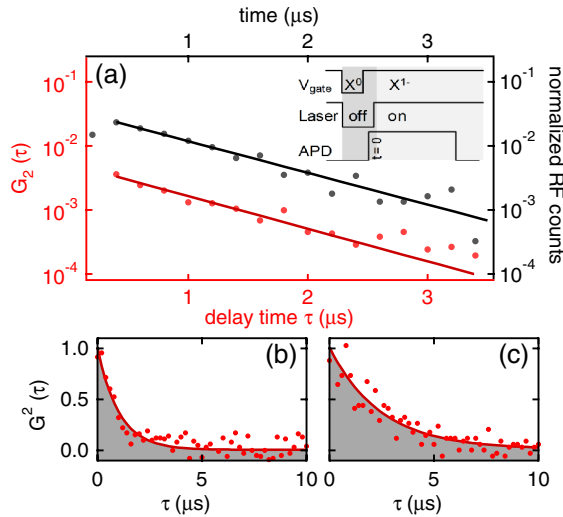
FIG. 3 (color online).   (a) G_2 (bottom) and nshot (top) measurements obtained at a gate voltage in the middle of the plateau and laser intensity $P = P_{sat}$. Solid lines are exponential fits with decay times (840 ± 40) ns and (860 ± 20) ns respectively, demonstrating the agreement between the two measurement methods. (b),(c) G_2 curves obtained from a second quantum dot with a laser power $P = 0.1 P_{sat}$ and at two gate voltages close to the plateau edge (large cotunneling) and 7.5 mV apart. The solid lines are exponential fits, showing decay times of (1.0 ± 0.1) μs and (2.5 ± 0.2) μs, respectively. These decay times are direct measurements of cotunneling-limited spin decay rates at the given gate voltages.

were increased such that $p_1 \sim 1.0$ were achieved, our scheme would constitute a single-shot QND measurement of the electron spin. We estimate that such a spin measurement [23] is within reach using our scheme. Collection efficiencies from microcavities have been predicted to be as high as 35% [24] which would in turn give up to a factor of 15 improvement in the overall collection efficiency. In addition, given the observation that a sizeable fraction of QDs have vanishing in-plane heavy-hole g factors [8], it is plausible to expect much smaller spin-flip spontaneous emission rate γ from the trion state, as to what we observed in our experiments. A smaller branching ratio will reduce the laser backaction allowing a nondemolition measurement to be performed on a longer time scale, and hence with better efficiency. By combining the above two factors, achieving a factor of more than 10 improvement in the measurement efficiency p_1 necessary for a single-shot QND measurement appears feasible.

A particularly exciting possible extension for the spin-photon interface demonstrated here is for a double-QD system consisting of a gate-defined and a self-assembled QD [25]. It has been shown that in a coupled-QD system, optical transitions in a neutral QD could be used to monitor the spin state of a single-electron charged QD [26]. If

realized, a double-QD spin-photon interface along the lines we describe in this Letter could be used to generate distant spin entanglement between two gated QDs. Another interesting extension is the implementation of our method in a single-hole charged QD where the positively charged trion transition selection rules are identical to the ones we considered [27].

[1] A. Imamoglu *et al.*, Phys. Rev. Lett. **83**, 4204 (1999).
[2] B. B. Blinov *et al.*, Nature (London) **428**, 153 (2004).
[3] A. N. Vamivakas *et al.*, Nature Phys. **5**, 198 (2009).
[4] E. B. Flagg *et al.*, Nature Phys. **5**, 203 (2009).
[5] C. Cabrillo *et al.*, Phys. Rev. A **59**, 1025 (1999).
[6] D. L. Moehring *et al.*, Nature (London) **449**, 68 (2007).
[7] D. F. Walls and G. J. Milburn, *Quantum Optics* (Springer, New York, 2008), 2nd ed.
[8] G. Fernandez *et al.*, Phys. Rev. Lett. **103**, 087406 (2009).
[9] M. Kaniber *et al.*, Phys. Rev. B **77**, 073312 (2008).
[10] K. Hennessy *et al.*, Nature (London) **445**, 896 (2007).
[11] M. T. Rakher *et al.*, Phys. Rev. Lett. **102**, 097403 (2009).
[12] D. Englund *et al.*, Opt. Express **17**, 18651 (2009).
[13] J. Dreiser *et al.*, Phys. Rev. B **77**, 075317 (2008).
[14] M. Atature *et al.*, Science **312**, 551 (2006).
[15] C. Latta *et al.*, Nature Phys. **5**, 758 (2009).
[16] C. -Y Lu *et al.*, Phys. Rev. B **81**, 035332 (2010).
[17] In the case of two nonidentical QDs, it would be advantageous to use the Voigt geometry, where one starts from an initial electron spin state $|\!\uparrow_x\rangle$ and upon scattering of a laser photon project the system onto the state $|\phi\rangle = (|\!\uparrow_x, 1_{\text{blue}}\rangle + |\!\downarrow_x, 1_{\text{red}}\rangle)/\sqrt{2}$. In this case, the energy difference between the blue and the red photons is determined exclusively by the electron Zeeman energy.
[18] E. B. Flagg *et al.*, Phys. Rev. Lett. **104**, 137401 (2010).
[19] X. Xu *et al.*, Phys. Rev. Lett. **99**, 097401 (2007).
[20] We emphasize that the average waiting time for achieving this single-photon-detection-based initialization is still ~ 10 μs for the Faraday geometry that we used.
[21] F. H. L. Koppens *et al.*, Nature (London) **442**, 766 (2006).
[22] M. A. Nielsen and I. L. Chuang, *Quantum Computation and Quantum Information* (Cambridge University Press, Cambridge, U.K., 2000).
[23] R. Hanson *et al.*, Rev. Mod. Phys. **79**, 1217 (2007).
[24] M. Larqué *et al.*, New J. Phys. **11**, 033022 (2009).
[25] H. A. Engel *et al.*, arXiv:cond-mat/0612700.
[26] D. Kim *et al.*, Phys. Rev. Lett. **101**, 236804 (2008).
[27] B. D. Gerardot *et al.*, Nature (London) **451**, 441 (2008).